DOCK2 deficiency mitigates HFD-induced obesity by reducing adipose tissue inflammation and increasing energy expenditure[S]

Xia Guo,* Feifei Li,*[†] Zaiyan Xu,*[§] Amelia Yin,**[††] Hang Yin,**[††] Chenxiao Li,* and Shi-You Chen[1],*

Departments of Physiology and Pharmacology,* Biochemistry and Molecular Biology,** and Center for Molecular Medicine,[††] University of Georgia, Athens, GA; Department of Cardiovascular Surgery,[†] Union Hospital, Wuhan, China; and College of Veterinary Medicine,[§] Huazhong Agricultural University, Wuhan, China

Abstract Obesity is the major risk factor for type 2 diabetes, cardiovascular disorders, and many other diseases. Adipose tissue inflammation is frequently associated with obesity and contributes to the morbidity and mortality. Dedicator of cytokinesis 2 (DOCK2) is involved in several inflammatory diseases, but its role in obesity remains unknown. To explore the function of DOCK2 in obesity and insulin resistance, WT and DOCK2-deficient (DOCK2$^{-/-}$) mice were given chow or high-fat diet (HFD) for 12 weeks followed by metabolic, biochemical, and histologic analyses. DOCK2 was robustly induced in adipose tissues of WT mice given HFD. DOCK2$^{-/-}$ mice with HFD showed decreased body weight gain and improved metabolic homeostasis and insulin resistance compared with WT mice. DOCK2 deficiency also attenuated adipose tissue and systemic inflammation accompanied by reduced macrophage infiltration. Moreover, DOCK2$^{-/-}$ mice exhibited increased expression of metabolic genes in adipose tissues with greater energy expenditure. Mechanistically, DOCK2 appeared to regulate brown adipocyte differentiation because increased preadipocyte differentiation to brown adipocytes in interscapular and inguinal fat was observed in DOCK2$^{-/-}$ mice, as compared with WT.[JLR] These data indicated that DOCK2 deficiency protects mice from HFD-induced obesity, at least in part, by stimulating brown adipocyte differentiation. Therefore, targeting DOCK2 may be a potential therapeutic strategy for treating obesity-associated diseases.—Guo, X., F. Li, Z. Xu, A. Yin, H. Yin, C. Li, and S-Y. Chen. **DOCK2 deficiency mitigates HFD-induced obesity by reducing adipose tissue inflammation and increasing energy expenditure.** *J. Lipid Res.* **2017.** 58: 1777–1784.

Obesity is a growing global public health challenge because of its association with a number of chronic diseases such as type 2 diabetes, hypertension, and other cardiovascular diseases (1). Obesity is mainly caused by a chronic imbalance between energy intake and expenditure resulting in increased adipose tissue mass (2). Because current pharmaceutical therapies often have adverse side effects or limited efficacy, it is important to identify and develop more effective therapeutics to treat obesity. Increasing evidence supports the pivotal role of adipose tissue in lipid storage, adipokine secretion, thermogenesis, and glucose homeostasis, thereby regulating energy balance (3). Although the underlying mechanism is not entirely understood, adipose tissue inflammation is frequently observed in diet-induced obesity in humans and rodents and is considered as one of the critical links between obesity and the accompanied insulin resistance in type 2 diabetes (4, 5).

Adipose tissue produces adipokines, including hormones, cytokines, and other molecules, to regulate the whole body metabolism by releasing them into the circulation. Adiponectin is a hormone solely expressed in differentiated adipocytes to regulate insulin sensitivity and obesity. Its expression is reduced in obesity and insulin-resistant conditions, but upregulated following weight loss (6). Leptin is another hormone secreted exclusively by adipocytes to

regulate energy balance by inhibiting hunger (7). Some secreted adipokines and chemokines are essential for the recruitment of immune cells, especially macrophages, to the adipose tissue (8, 9). The adipose tissue macrophages are a major source of proinflammatory cytokines and chemokines, including interleukin (IL)-6, TNF-α, monocyte chemoattractant protein 1 (MCP-1), and IL-12. These cytokines eventually lead to insulin resistance and metabolic disorders (10, 11). For instance, TNF-α has been shown to modulate insulin sensitivity in obesity by inhibiting insulin signaling in adipocytes. TNF-α can also induce adipocyte apoptosis and stimulate lipolysis by decreasing expression of lipolysis-inhibiting Gi protein (12, 13). Blocking the function of proinflammatory cytokines or chemokines has been shown to improve insulin sensitivity and glucose homeostasis (12). Three types of adipose tissues have been identified in mammals, namely brown, brite (brown-in-white), and white adipose tissues, which express genes regulating adipogenesis and lipid storage [PPAR-α/γ and cell death-inducing DFFA-like effector a (Cidea)], lipolysis [hormone-sensitive lipase (HSL)], or energy expenditure [uncoupling protein 1 (UCP1)] (14).

Dedicator of cytokinesis 2 (DOCK2) is an atypical guanine nucleotide exchange factor (GEF) for the Rho-small guanine triphosphatase mainly expressed in hematopoietic cells that regulates lymphocyte activation and migration (15). DOCK2 also controls various immunological functions including helper T cell differentiation, neutrophil chemotaxis, and type I interferon induction (16). Recently, we found that DOCK2 modulates SMC phenotype by inhibiting myocardin-mediated SMC gene transcription (17). Because DOCK2 knockout (DOCK2$^{-/-}$) mice are smaller compared with the WT controls, we postulated that DOCK2 might play a role in the metabolism of mice. Indeed, we found that DOCK2 was significantly upregulated in adipose tissues of mice fed high-fat diet (HFD). DOCK2 deficiency, however, attenuated the HFD-caused body weight gain. DOCK2 deficiency also improved metabolic homeostasis and insulin resistance in HFD-fed mice. Moreover, DOCK2$^{-/-}$ mice showed increased energy expenditure with upregulation of metabolic genes and accumulation of more brown/beige adipocytes in interscapular and inguinal fat depots, which was due to an increased brown adipogenic differentiation.

MATERIALS AND METHODS

Animals and diets

All animals were housed under conventional conditions in the animal care facilities and received humane care in compliance with the Principles of Laboratory Animal Care formulated by the National Society for Medical Research and the National Institutes of Health *Guide for the Care and Use of Laboratory Animals*. All experimental procedures were approved by the IACUC of the University of Georgia. WT C57BL/6 mice were purchased from the Jackson Laboratory. DOCK2$^{-/-}$ mice on the C57BL/6 background were reported previously (17, 18). The age-matched WT and DOCK2$^{-/-}$ male mice were maintained on a 12 h light/dark cycle with free access to regular chow for 8 weeks. The mice were then fed either chow (25% protein, 62% carbohydrate, and 13% fat; 3.07 kcal/g; 5053, LabDiet) or HFD (20% protein, 40% carbohydrate, and 40% fat; 4.5 kcal/g; D12108C, Research Diets) for an additional 12 weeks. At the end of the feeding, mice were fasted overnight and anesthetized with 2.0% isoflurane. Blood was collected by direct cardiac puncture and serum was prepared by centrifugation of blood at 4,000 g for 10 min at 4°C and stored at −80°C for later analyses. Epididymal, inguinal, and interscapular fat depots were carefully removed and weighed. A portion of the fat was fixed in 4% paraformaldehyde for histological analysis and the remaining fat was stored at −80°C for RNA and protein preparation.

Body weight and energy expenditure measurement

Body weight was measured every week, and the food intake in different mouse groups was recorded accordingly. The energy expenditure of an individual mouse was measured for 7 days using metabolic cages (Oxymax; Columbus Instruments, Columbus, OH). Briefly, mice were fed HFD for 2 weeks, maintained at 20–24°C on a 12 h light/12 h dark cycle. Heat, VO$_2$, VCO$_2$, and respiratory exchange ratio (RER) were measured while physical activities were recorded.

Cell culture

C3H10T1/2 cells (ATCC) were cultured in DMEM (catalog number 45000-316; VWR) supplemented with 10% FBS (catalog number S11550; Atlanta Biologicals) and treated with 6.3 nM rhBMP7 (catalog number 354-BP-010; R&D Systems) for 3 days. The confluent cells were induced to differentiate in 10% FBS, 860 nM insulin (catalog number: I9278; Sigma-Aldrich), 1 nM 3,3,5-triiodo-L-thyronine (T3) (catalog number T2877; Sigma-Aldrich), 5 mM dexamethasone (catalog number D4902; Sigma-Aldrich), 0.5 mM 3-isobutyl-methylxanthine (catalog number I5879; Sigma-Aldrich), and 125 mM indomethacin (catalog number I7378; Sigma-Aldrich). Two days after induction, cells were maintained in 10% FBS, insulin, and T3 for 6 days (19). To culture preadipocytes, interscapular and inguinal fat pads from eight-week-old mice were excised, minced, and digested in collagenase (catalog number 234155; Sigma-Aldrich) at 37°C for 40 min. Then, the digested fat tissues were filtered through a 100 μm nylon mesh and centrifuged at 900 g for 5 min. The pellet was resuspended in DMEM supplemented with 10% FBS and cultured in a 6 cm cell culture dish. Medium was changed the next day and then every 2 days. When cells were grown to confluence, culture medium was changed to DMEM containing 10% FBS, 2.85 μM insulin, 0.3 μM dexamethasone, 0.63 mM 3-isobutyl-methylxanthine, and 1 μM rosiglitazone (catalog number R2408; Sigma-Aldrich) to induce for 3 days. Cells were then differentiated in differentiation medium containing DMEM with 10% FBS, 200 nM insulin, and 10 nM T3 for 4 days until adipocytes matured (20).

RNA extraction and real-time quantitative PCR

RNA extraction from epididymal, interscapular, and inguinal fat tissues was performed as described previously (21, 22). Total RNA was isolated using Trizol reagent. Quantitative (q)PCR assessing gene expression was performed in an Mx3005P qPCR machine using SYBR Green master mix (catalog number QP005; Genecopoeia) as described previously (21). Each sample was amplified in triplicate. The primer sequences for the involved genes are included in the supplemental Table S1.

Western blot analysis

Protein extraction and Western blot (WB) procedures were described previously (17). Antibodies against DOCK2 (catalog

number 09-454; Millipore), F4/80 (catalog number ab6640; Abcam), HSL (catalog number 4107S; Cell Signaling Technology), PPAR-α, (catalog number ab8934; Abcam), PPAR-γ coactivator 1α (PGC1α) (catalog number ab54481; Abcam), UCP1 (catalog number ab10983; Abcam), PR domain containing 16 (PRDM16) (catalog number ab106410; Abcam), GAPDH (catalog number G8795; Sigma), and α-tubulin (catalog number T5168; Cell Signaling Technology) were used for immunoblotting. Protein expressions were detected using an enhanced chemiluminescence kit (catalog number WBKLS0500; Millipore).

Glucose and insulin tolerance tests

For the glucose tolerance test (GTT), mice were fasted overnight followed by an intraperitoneal injection of glucose (1 g/kg body weight; catalog number G7021; Sigma-Aldrich). Blood glucose levels were measured by venous tail bleeding using the One-Touch AccuChek glucometer (Roche) at 0, 15, 30, 60, and 120 min. The insulin tolerance test (ITT) was performed without fast. Mice were injected intraperitoneally with insulin (1.5 IU/kg body weight) and blood glucose was measured at 0, 15, 30, 60, and 120 min.

Blood biochemical analysis

Plasma triglyceride (TG), total cholesterol (TC), HDL cholesterol, LDL/VLDL cholesterol, adiponectin, and leptin were measured with a TG quantification kit (catalog number ab65336; Abcam), an HDL and LDL/VLDL cholesterol assay kit (catalog number ab65390; Abcam), an adiponectin mouse ELISA kit (catalog number ab108785; Abcam), and a leptin mouse ELISA kit (catalog number ab100718; Abcam), respectively. Fasting plasma levels of glucose and insulin were measured with a One-Touch AccuChek glucometer and a rat/mouse insulin ELISA kit (catalog number EZRMI-13K; Millipore), respectively. The homeostasis model assessment of insulin resistance (HOMA-IR) was calculated as described previously (23). Plasma levels of inflammatory markers were assayed using a cytometric bead array mouse inflammation kit (catalog number BDB552364; BD Biosciences) following the manufacturer's instructions. Data were collected by FACSCalibur flow cytometer (Becton Dickinson).

Histological and immunohistochemistry staining

Mouse adipose tissues were fixed in 4% paraformaldehyde, dehydrated, and embedded in paraffin. Sections (5 μm) were cut, deparaffinized, and stained with H&E using standard protocol. Images were captured using a Nikon microscope. For quantitative analysis of adipocyte area, eight images of H&E-stained sections were acquired from each animal, and the cross-sectional area of adipocytes was measured using ImageJ software. The expression of DOCK2, F4/80, PGC1α, UCP1, and PRDM16 in adipose tissues was assessed by immunohistochemistry (IHC) staining using their corresponding antibodies.

Statistical analysis

GraphPad Prism 5 was used for statistical analyses. Data were evaluated with a two-tailed unpaired Student's *t*-test or compared by one-way ANOVA followed by Fisher's *t*-test. Data are expressed as mean ± SD. A value of $P < 0.05$ was considered statistically significant.

RESULTS

DOCK2 deficiency inhibited obesity development with a reduction of fat mass in HFD-fed mice

To test whether DOCK2 is involved in HFD-induced obesity, we first fed WT mice HFD for 12 weeks to detect

DOCK2 expression in epididymal adipose tissue. As shown in **Fig. 1A**–C, DOCK2 was significantly induced by HFD at both mRNA and protein levels. IHC staining showed that there was no detectable level of DOCK2 in adipose tissue of WT mice fed chow, while HFD dramatically upregulated its expression (Fig. 1D, E). Importantly, DOCK2 deficiency dramatically inhibited HFD-induced increase in epididymal fat weight as compared with WT mice (Fig. 1F). Consequently, although WT mice fed HFD showed a significant increase in body weight, DOCK2 deficiency diminished the weight gain (Fig. 1G). Because the fat weight increase and consequent obesity could have been due to adipocyte hyperplasia or hypertrophy, we observed the adipocyte size and numbers in WT and DOCK2$^{-/-}$ mice. Unlike HFD-fed WT mice that displayed adipocyte hypertrophy, HFD-fed DOCK2$^{-/-}$ mice preserved a normal adipocyte size (Fig. 1H, I), similar to the lean mice. These results indicated that DOCK2 deficiency diminished obesity development by reducing HFD-increased fat mass.

DOCK2 deficiency improved metabolic homeostasis and insulin resistance in HFD-fed mice

Significantly higher serum concentrations of TG, TC, HDL, and LDL/VLDL were observed in WT mice fed HFD as compared with the regular chow (**Fig. 2A**–D). However, DOCK2 deficiency attenuated the elevation in serum TG and cholesterol induced by HFD (Fig. 2A–D). Importantly, although there was no significant difference in fasting blood glucose and insulin levels between WT and DOCK2$^{-/-}$
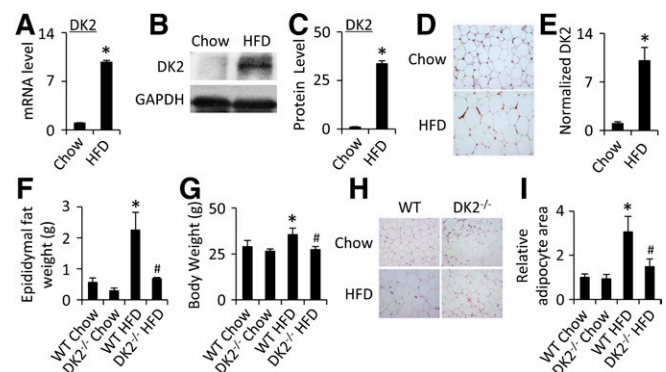

Fig. 1. DOCK2 deficiency prevented mice from HFD-induced obesity. A: HFD (12 weeks) increased DOCK2 (DK2) mRNA expression, as detected by qPCR. *$P < 0.05$ versus chow group (n = 3). B: HFD increased DK2 protein expression as detected by WB. C: Quantification of DK2 protein levels shown in (B) by normalizing to GAPDH. *$P < 0.05$ versus chow group (n = 3). D: IHC staining showed DK2 induction in adipose tissue of HFD-fed mice. E: Quantification of DK2 levels shown in (D). *$P < 0.05$ versus chow group (n = 6–8). F: Weights of epididymal fat in WT and DOCK2 knockout (DK2$^{-/-}$) mice fed chow or HFD for 12 weeks. *$P < 0.05$ versus WT chow group, #$P < 0.05$ versus WT HFD group (n = 6–8). G: Body weight of WT and DOCK2$^{-/-}$ mice fed with chow or HFD for 12 weeks. *$P < 0.05$ versus WT chow group, #$P < 0.05$ versus WT HFD group (n = 6–8). H: Morphology of epididymal fat from WT and DK2$^{-/-}$ mice fed chow or HFD as shown by H&E staining. I: Quantification of the mean adipocyte size shown in (H) by measuring the cross-section area. The areas were relative to the mean cross-section area of adipocytes from WT mice fed chow (set as 1). *$P < 0.05$ versus WT chow group, #$P < 0.05$ versus WT HFD group (n = 6–8).
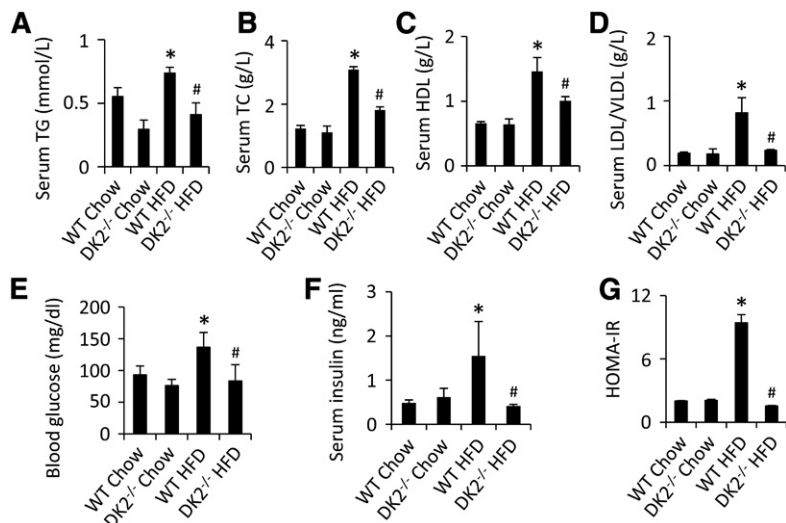
Fig. 2. DOCK2 deficiency restored metabolic homeostasis in HFD-fed mice. Serum TG (A), serum TC (B), HDL cholesterol (C), and LDL/VLDL cholesterol (D) concentrations in WT and DOCK2$^{-/-}$ mice fed normal chow or HFD were measured by ELISA. Fasting blood glucose (E), insulin concentration (F), and HOMA-IR (HOMA-IR = fasting glucose × fasting insulin/22.5) (G) in WT and DOCK2$^{-/-}$ mice fed normal chow or HFD were measured as described in the Materials and Methods. *$P < 0.05$ versus WT chow group, #$P < 0.05$ versus WT HFD group (n = 6–8).

mice fed regular chow (Fig. 2E, F), HFD significantly increased the fasting blood glucose level, insulin concentration, and HOMA-IR score in WT mice, but not in DOCK2$^{-/-}$ mice (Fig. 2E–G). These data were consistent with results of the ITT and GTT. DOCK2 deficiency improved glucose tolerance and insulin sensitivity, as evidenced by the decreased area under the curve (AUC) of the ITT and GTT, as compared with HFD-fed WT mice (**Fig. 3A**–D). These data demonstrated that DOCK2 deficiency improved glucose tolerance and protected mice from HFD-induced insulin resistance.

DOCK2 deficiency attenuated adipose tissue and systemic inflammation in HFD-fed mice

Adipose tissue and systemic inflammation contribute to the development of obesity. Therefore, we detected the expression of the proinflammatory cytokines, adiponectin, leptin, IL-6, IL-10, TNF-α, and IL-12, in the adipose tissues and serum of WT and DOCK2$^{-/-}$ mice fed HFD. Adiponectin is an adipocyte-derived hormone that enhances insulin sensitivity, improves fatty acid oxidation, and suppresses hepatic gluconeogenesis (24, 25). Although there was no significant difference in serum concentration of adiponectin between WT and DOCK2$^{-/-}$ mice, DOCK2 deficiency increased adiponectin expression in the fat tissue (**Fig. 4A**, D). Moreover, DOCK2 deficiency significantly decreased the expression of leptin, IL-6, IL-10, TNF-α, and IL-12 in fat tissue as compared with WT mice (Fig. 4B, C). Because fat accumulation in obese mice is usually accompanied by low-grade systemic inflammation, we further examined the inflammatory status in the blood circulation of HFD-fed DOCK2$^{-/-}$ mice. As shown in Fig. 4E, F, the plasma levels of the inflammatory cytokines, leptin, IL-6, IL-10, TNF-α, and IL-12, were much lower in HFD-fed DOCK2$^{-/-}$ mice than in the WT obese mice. These data indicated that DOCK2 may be involved in the adipose tissue and systemic inflammation during the development of obesity.

To further explore the adipose tissue inflammation, we examined the macrophage accumulation in adipose tissues of WT and DOCK2$^{-/-}$ mice fed chow or HFD by detecting

the macrophage marker, F4/80. As shown in **Fig. 5A–C**, HFD upregulated the mRNA and protein expression of F4/80 in adipose tissue of WT mice, but not in DOCK2$^{-/-}$ mice. IHC staining showed that DOCK2 deficiency significantly decreased the number of F4/80-positive macrophages that were accumulated in adipose tissue with HFD (Fig. 5D). To further confirm the macrophage accumulation in adipose tissue, a different macrophage marker, i.e., CD68, was detected. As shown in Fig. 5E, HFD induced CD68 mRNA expression in adipose tissue, but DOCK2 deficiency inhibited CD68 expression. MCP-1 is known to play a critical role in mediating macrophage infiltration (26). Consistent with the macrophage infiltration in adipose tissue of HFD-fed mice, a 20-fold increase of MCP-1 expression was observed in adipose tissue of WT mice fed HFD compared with chow (Fig. 5F). DOCK2 deficiency, however,
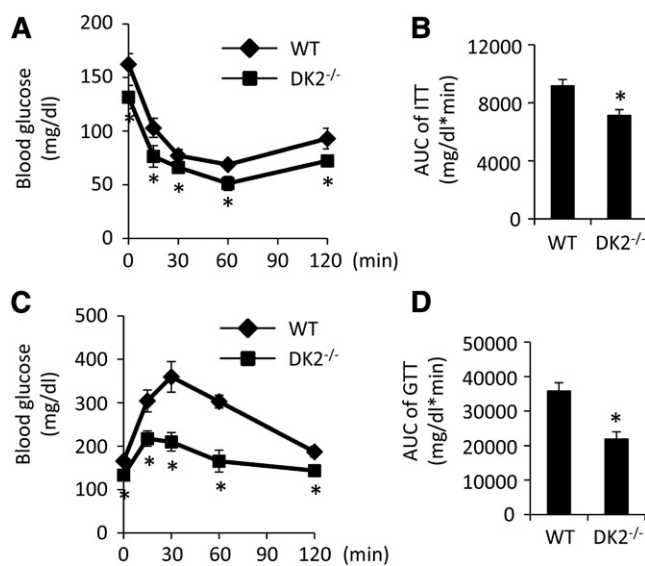

Fig. 3. DOCK2 deficiency prevented HFD-induced insulin resistance. A: ITT in WT and DOCK2$^{-/-}$ mice fed HFD. B: Inverse AUC of ITT. C: GTT in WT and DOCK2$^{-/-}$ mice fed HFD. D: Quantification of the AUC shown in (C). *$P < 0.05$ versus WT mice (B, D) or at each time point (A, C), respectively (n = 6).
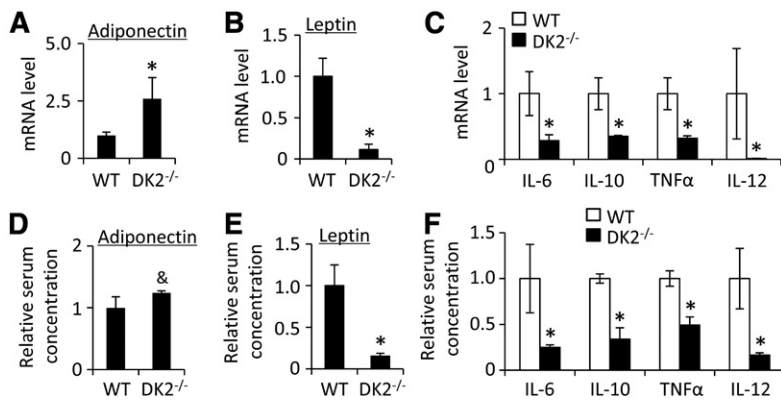
Fig. 4. DOCK2 deficiency attenuated HFD-induced adipose tissue and systemic inflammation. WT or DOCK2 knockout (DK2$^{-/-}$) mice fed HFD for 12 weeks. A–C: mRNA expression of adiponectin (A), leptin (B), and IL-6, IL-10, TNF-α, and IL-12 (C) in epididymal adipose tissue was measured by qPCR. D, E: Plasma concentrations of adiponectin (D) and leptin (E) were measured by ELISA using an adiponectin assay kit and a leptin assay kit, respectively. F: Plasma concentrations of IL-6, IL-10, TNFα, and IL-12 were measured by cytometric bead array immunoassay. *$P < 0.05$; &$P > 0.05$ versus WT mice for each corresponding gene, respectively (n = 6).

abolished the HFD-induced MCP-1 expression (Fig. 5F). DOCK2 deficiency also diminished the plasma MCP-1 level that was increased by HFD (Fig. 5G). These data suggested that DOCK2 deficiency may prevent HFD-induced macrophage accumulation in adipose tissues by inhibiting MCP-1 expression.

DOCK2 deficiency increased the expression of metabolic genes in adipose tissue along with greater energy expenditure

Because HFD-fed DOCK2$^{-/-}$ mice had a lean phenotype, we detected the expression of metabolic genes related to β-oxidation, lipolysis, and thermogenesis, such as PPAR-α, HSL, and PGC1α in adipose tissues from WT and DOCK2$^{-/-}$ mice fed with HFD. As shown in **Fig. 6A–E**, DOCK2 deficiency significantly increased the mRNA and protein levels of PPAR-α, HSL, and PGC1α in epididymal adipose tissue compared with WT, suggesting that DOCK2 may contribute to obesity by reducing β-oxidation, lipolysis, and thermogenesis. Because increased fat mass results mainly from excessive energy storage due to the excessive energy intake and lower energy expenditure, we measured the energy intake and expenditure by indirect calorimetry. The lean phenotype of HFD-fed DOCK2$^{-/-}$ mice was likely independent of energy intake because the food intake was similar in WT and DOCK2$^{-/-}$ mice fed with HFD (Fig. 6F).

There was also no significant difference in physical activity in WT and DOCK2$^{-/-}$ mice (Fig. 6G). Indirect calorimetry analyses of mice given HFD for 2 weeks showed that DOCK2$^{-/-}$ mice produced more heat, consumed more oxygen, and generated more carbon dioxide as compared with WT mice (Fig. 6H, supplemental Fig. S1). However, there were no significant differences in RER between the WT and DOCK2$^{-/-}$ mice, suggesting that the increased energy expenditure was the primary cause of reduced obesity in HFD-fed DOCK2$^{-/-}$ mice.

DOCK2 deficiency induced brown adipocyte differentiation

Brown adipose tissue (BAT) is closely related to the increased energy expenditure, and PGC1α is a critical factor regulating the proliferation and differentiation of BAT (27). Therefore, we sought to determine the BAT markers in the interscapular and inguinal fat tissues of WT and DOCK2$^{-/-}$ mice fed with HFD. As shown in **Fig. 7A–D**, the protein expression of the BAT markers, PGC1α, UCP1, and Prdm16, (Fig. 7A–D) was increased in both interscapular (Fig. 7A, B) and inguinal fat tissues (Fig. 7C, D) of DOCK2$^{-/-}$ mice compared with WT. IHC staining of interscapular adipose tissue confirmed the increased expression of PGC1α, UCP1, and Prdm16 in interscapular adipose tissue (Fig. 7E, F). These data indicated that DOCK2 deficiency
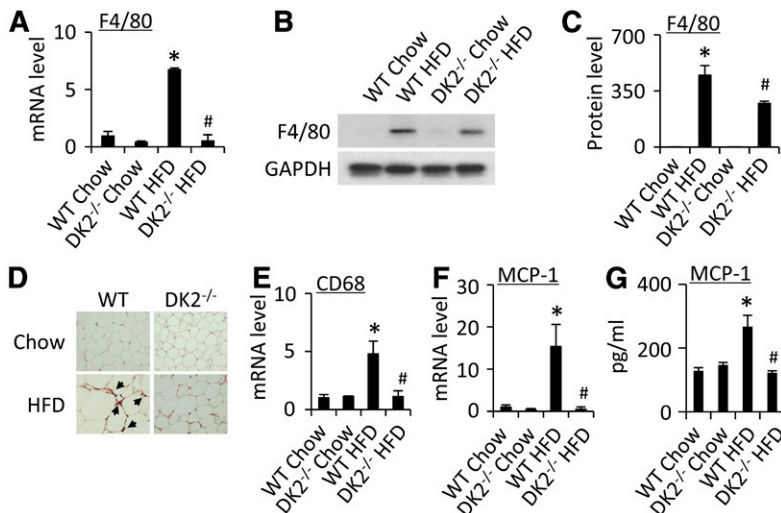

Fig. 5. DOCK2 deficiency attenuated macrophage infiltration in adipose tissue of HFD-fed mice. Epididymal adipose tissues from WT and DOCK2 knockout (DK2$^{-/-}$) mice fed chow or HFD for 12 weeks were used for gene expression analyses. A: F4/80 mRNA expression was measured by qPCR. B: F4/80 protein expression was detected by WB. C: Quantification of F4/80 protein level shown in (B) by normalizing to GAPDH. D: IHC staining showed the F4/80-positive cells (arrowhead). E, F: CD68 (E) and MCP-1 (F) mRNA expression was measured by qPCR. G: Plasma MCP-1 was measured by ELISA. *$P < 0.05$ versus WT chow group, #$P < 0.05$ versus WT HFD group (n = 6).
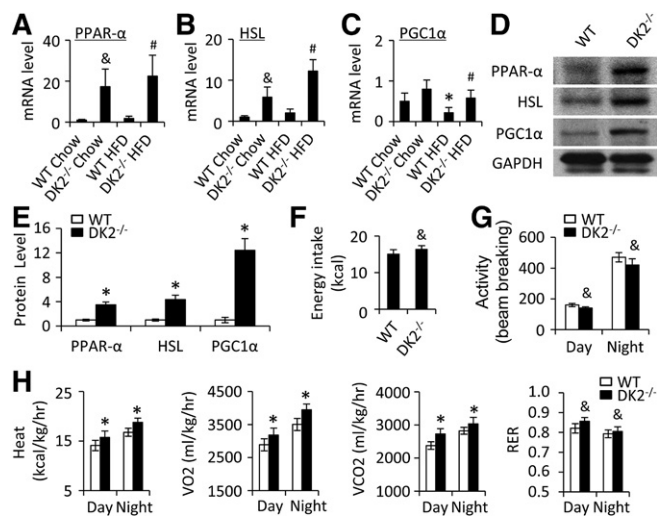
DOCK2 in obesity and insulin resistance   1781

Fig. 6. DOCK2 deficiency caused the increased expression of metabolic genes in adipose tissue and greater energy expenditure. A–C: mRNA expression of PPAR-α (A), HSL (B), and PGC1α (C) in epididymal adipose tissue from WT and DOCK2$^{-/-}$ mice. $^{\&}P < 0.05$ versus WT chow group; $^{\#}P < 0.05$ versus WT HFD group; $^{*}P < 0.05$ versus WT chow group (n = 6). D: PPAR-α, HSL, and PGC1α protein expression in epididymal adipose tissue in WT and DOCK2$^{-/-}$ mice fed with HFD were detected by WB. E: Quantification of protein levels shown in (D) by normalizing to GAPDH. *$P < 0.05$ versus WT HFD group for each corresponding protein (n = 3). F: Energy intake of WT and DOCK2$^{-/-}$ mice fed on HFD. G, H: WT and DOCK2$^{-/-}$ mice were given HFD for 2 weeks and housed in a computer-controlled open-circuit indirect calorimeter to measure physical activity (G), heat production, oxygen consumption (VO2), CO2 production (VCO2), and RER (H) during a 12 h dark and light cycle. RERs were calculated by volume of carbon dioxide produced (exhaled)/volume of oxygen consumed (inhaled). *$P < 0.05$; $^{\&}P > 0.05$ versus WT mice (n = 6).

Fig. 7. DOCK2 deficiency increased brown adipocytes in interscapular and inguinal fat tissues. WT and DOCK2 knockout (DK2$^{-/-}$) mice were fed HFD for 12 weeks. A–D: PGC1α, UCP1, and PRDM16 protein levels in interscapular (A, B) and inguinal (C, D) adipose tissues were detected by WB. Protein levels shown in (A) (B) and (C) (D) were quantified by normalizing to GAPDH in (A) and (C), respectively. *$P < 0.05$ versus WT group for each corresponding protein, respectively (n = 3). E: PGC1α, UCP1, and PRDM16 expression in interscapular adipose tissues were detected by IHC. F: Quantification of the protein levels shown in (G) by measuring the staining intensity. *$P < 0.05$ versus WT group (n = 6).

might increase BAT content, leading to the increased energy expenditure.

Because DOCK2 is involved in cell differentiation, we tested to determine whether DOCK2 regulates adipocyte differentiation. C3H10T1/2 cells are beige adipocyte progenitors because BMP7 and other differentiation factors can induce C3H10T1/2 cells to become brown-like adipocytes (19). DOCK2 was downregulated during the differentiation of C3H10T1/2 cells (**Fig. 8A**). BMP7 and differentiation agents indeed induced the differentiation of C3H10T1/2 cells to adipocytes, as shown by the acquired adipocyte phenotype (Fig. 8B) and the expression of adipocyte markers, Cidea, PGC1α, and PPAR-γ (Fig. 8C). Forced expression of DOCK2, however, significantly inhibited the differentiation, as indicated by the reversal of adipocyte phenotype and adipocyte marker expression (Fig. 8B, C). To test DOCK2 function in brown adipocyte differentiation in fat tissues, we cultured preadipocytes from interscapular and inguinal fat tissues of WT and DOCK2$^{-/-}$ mice and induced their differentiation. As shown in Fig. 8D, E, DOCK2 deficiency significantly increased the expression of Cidea and PGC1α in interscapular preadipocytes (Fig. 8D), while enhancing Cidea and UCP1 expression in inguinal preadipocytes (Fig. 8E), as compared with the WT preadipocytes. These data indicated that the increased
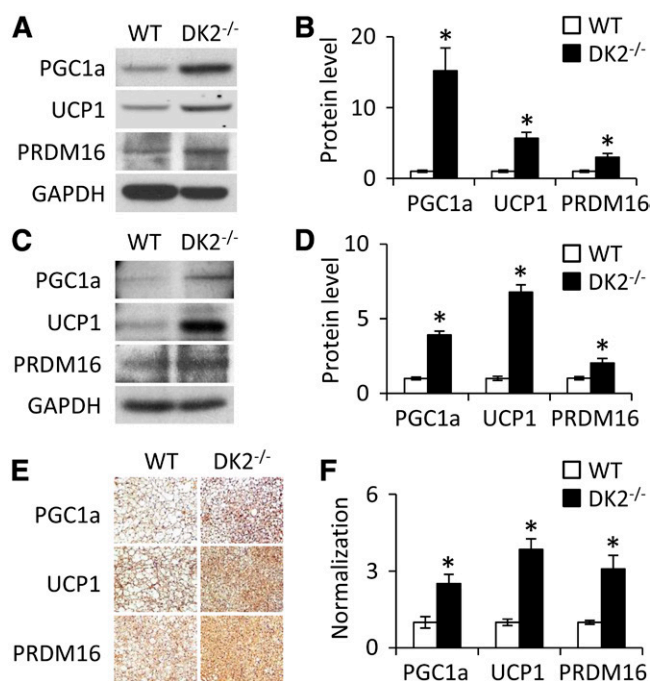
energy expenditure observed in DOCK2$^{-/-}$ was due, at least in part, to the increased brown adipocyte differentiation.

DISCUSSION

Our current studies demonstrate that DOCK2 deficiency leads to beneficial effects including reduced adipose tissue hypertrophy, attenuated adipose tissue inflammation, and improved insulin sensitivity in HFD-fed mice. DOCK2 is undetectable in mouse adipose tissue, but is robustly induced during the development of HFD-induced obesity. Importantly, DOCK2 deficiency improves metabolic homeostasis by normalizing the HFD-induced increase of plasma TG, TC, HDL, and LDL/VLDL. Moreover, DOCK2 deficiency attenuates HFD-increased fasting blood glucose level, insulin concentration, and HOMA-IR score. Thus, DOCK2 is likely an important factor regulating the development of obesity.

Several mechanisms are involved in the development of obesity and the accompanied insulin resistance. The increased inflammation in adipose tissue and low-grade system inflammation appear to be important (28). DOCK2 regulates lymphocyte activation and various immunological functions indicating a vital role in regulating inflammation (16). Indeed, the attenuation of diet-induced obesity
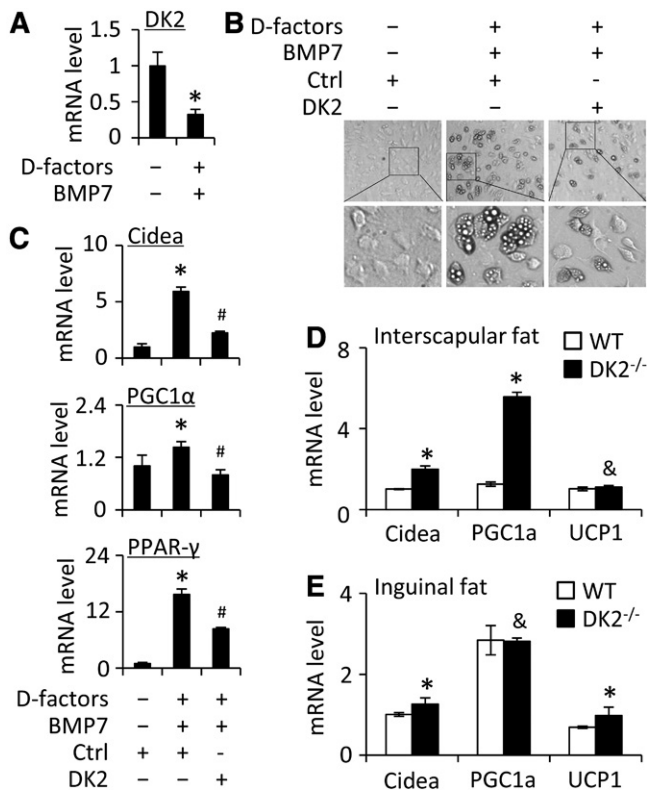
Fig. 8. DOCK2 deficiency increased brown adipocyte differentiation. A: mRNA expression of DOCK2 in C3H10T1/2 cells exposed to vehicle or differentiation factors (D-factors) and BMP7. *$P < 0.05$ versus vehicle-treated group ($-$) (n = 3). B: Cell morphological alteration of C3H10T1/2 cells after adipocyte differentiation. Cells were transfected with empty vector (Ctrl) or DOCK2 expression plasmid (DK2) followed by treatment with vehicle ($-$) or D-factors and BMP7, as indicated. C: mRNA expression of Cidea, PGC1α, and PPAR-γ in C3H10T1/2 cells after differentiation. Cells were treated similarly as in (B). *$P < 0.05$ versus vehicle group ($-$), #$P < 0.05$ versus empty vector (Ctrl)-transfected cells treated with D-factors and BMP7 (n = 3). D, E: Preadipocytes were isolated from interscapular adipose tissues (D) and inguinal adipose tissues (E) of WT or DOCK2 knockout (DK2$^{-/-}$) mice. The cells were exposed to differentiation factors in order to induce brown adipocytes. mRNA expression of Cidea, PGC1α, and UCP1 was detected by qPCR. *$P < 0.05$ versus WT group, &$P > 0.05$ versus WT (n = 3).

in DOCK2$^{-/-}$ mice is associated with the reduced adipose tissue and systemic inflammation. DOCK2 deficiency reduces the production of proinflammatory adipokines including adiponectin, leptin, IL-6, IL-10, TNF-α, and IL-12 in adipose tissue as well as in plasma. It is known that macrophage infiltration contributes to the development of obesity (29). The decreased adipose tissue inflammation may be attributable to the reduced macrophage accumulation, while the reduction in the systemic inflammation may be caused by DOCK2 function in different inflammatory cells in addition to macrophages.

In addition to adipose tissue inflammation, DOCK2 appears to also regulate the expression of a number of genes involved in metabolism. PPAR-α is a transcription factor regulating the expression of numerous genes related to lipoprotein transport, fatty acid uptake and binding, mitochondrial β-oxidation, and peroxisomal β-oxidation in fat

cells (30). HSL is the major lipase to cleave fatty acids from the TG molecule. The adipocyte HSL activity and expression is often decreased in obese subjects (31). PGC1α is a transcription coactivator interacting with numerous transcription factors to regulate adaptive thermogenesis, mitochondrial biogenesis, and fatty acid metabolism (32). DOCK2 deficiency upregulates the expression of PPAR-α, HSL, and PGC1α, suggesting that DOCK2 may regulate the obesity development by influencing the thermogenesis. Indeed, the lean phenotype of HFD-fed DOCK2$^{-/-}$ mice is correlated with the increased energy expenditure independent of energy intake and physical activity.

BAT contains a high amount of mitochondria that are functionalized by UCP1 that mediates nonshivering thermogenesis (33). Thus, BAT may curb obesity development by increasing energy expenditure. DOCK2 deficiency appears to enhance BAT markers, as shown by the increased expression of PGC1α and UCP1 in the interscapular and inguinal fat tissues of HFD-fed DOCK2$^{-/-}$ mice. Prdm16, a brown adipose determination factor, is also highly expressed in interscapular and inguinal fat tissues in HFD-fed DOCK2$^{-/-}$ mice. The increased BAT content in HFD-fed DOCK2$^{-/-}$ mice is due, at least in part, to the enhanced differentiation of brown adipocytes because forced expression of DOCK2 inhibits, while DOCK2 deficiency promotes, the brown adipocyte differentiation from adipocyte progenitors or preadipocytes isolated from interscapular and inguinal fat.

Taken together, our studies have demonstrated that DOCK2 deficiency protects mice from HFD-induced obesity, metabolic disorders, and insulin resistance by attenuating adipose tissue inflammation and increasing energy expenditure in adipose tissues. These pivotal roles of DOCK2 in obesity indicate that targeting DOCK2 may be a potential therapeutic strategy for treating obesity-associated diseases.

REFERENCES

1. Goran, M. I., G. D. Ball, and M. L. Cruz. 2003. Obesity and risk of type 2 diabetes and cardiovascular disease in children and adolescents. *J. Clin. Endocrinol. Metab.* **88:** 1417–1427.
2. Stunkard, A. J. 1996. Current views on obesity. *Am. J. Med.* **100:** 230–236.
3. Berg, A. H., and P. E. Scherer. 2005. Adipose tissue, inflammation, and cardiovascular disease. *Circ. Res.* **96:** 939–949.
4. Weisberg, S. P., D. McCann, M. Desai, M. Rosenbaum, R. L. Leibel, and A. W. Ferrante, Jr. 2003. Obesity is associated with macrophage accumulation in adipose tissue. *J. Clin. Invest.* **112:** 1796–1808.
5. Xu, H., G. T. Barnes, Q. Yang, G. Tan, D. Yang, C. J. Chou, J. Sole, A. Nichols, J. S. Ross, L. A. Tartaglia, et al. 2003. Chronic inflammation in fat plays a crucial role in the development of obesity-related insulin resistance. *J. Clin. Invest.* **112:** 1821–1830.
6. Havel, P. J. 2002. Control of energy homeostasis and insulin action by adipocyte hormones: leptin, acylation stimulating protein, and adiponectin. *Curr. Opin. Lipidol.* **13:** 51–59.
7. Mantzoros, C. S. 2001. The role of leptin and hypothalamic neuropeptides in energy homeostasis: update on leptin in obesity. *Growth Horm. IGF Res.* **11 (Suppl. A):** S85–S89.
8. Bai, Y., and Q. Sun. 2015. Macrophage recruitment in obese adipose tissue. *Obes. Rev.* **16:** 127–136.
9. Oh, D. Y., H. Morinaga, S. Talukdar, E. J. Bae, and J. M. Olefsky. 2012. Increased macrophage migration into adipose tissue in obese mice. *Diabetes.* **61:** 346–354.

10. Lee, J. 2013. Adipose tissue macrophages in the development of obesity-induced inflammation, insulin resistance and type 2 diabetes. *Arch. Pharm. Res.* **36:** 208–222.

11. Olefsky, J. M., and C. K. Glass. 2010. Macrophages, inflammation, and insulin resistance. *Annu. Rev. Physiol.* **72:** 219–246.

12. Uysal, K. T., S. M. Wiesbrock, M. W. Marino, and G. S. Hotamisligil. 1997. Protection from obesity-induced insulin resistance in mice lacking TNF-alpha function. *Nature.* **389:** 610–614.

13. Botion, L. M., A. R. Brasier, B. Tian, V. Udupi, and A. Green. 2001. Inhibition of proteasome activity blocks the ability of TNF alpha to down-regulate G(i) proteins and stimulate lipolysis. *Endocrinology.* **142:** 5069–5075.

14. Bi, P., T. Shan, W. Liu, F. Yue, X. Yang, X. R. Liang, J. Wang, J. Li, N. Carlesso, X. Liu, et al. 2014. Inhibition of Notch signaling promotes browning of white adipose tissue and ameliorates obesity. *Nat. Med.* **20:** 911–918.

15. Nishihara, H., S. Kobayashi, Y. Hashimoto, F. Ohba, N. Mochizuki, T. Kurata, K. Nagashima, and M. Matsuda. 1999. Non-adherent cell-specific expression of DOCK2, a member of the human CDM-family proteins. *Biochim. Biophys. Acta.* **1452:** 179–187.

16. Guo, X., and S. Y. Chen. 2017. Dedicator of cytokinesis 2 in cell signaling regulation and disease development. *J. Cell. Physiol.* **232:** 1931–1940.

17. Guo, X., N. Shi, X. B. Cui, J. N. Wang, Y. Fukui, and S. Y. Chen. 2015. Dedicator of cytokinesis 2, a novel regulator for smooth muscle phenotypic modulation and vascular remodeling. *Circ. Res.* **116:** e71–e80.

18. Fukui, Y., O. Hashimoto, T. Sanui, T. Oono, H. Koga, M. Abe, A. Inayoshi, M. Noda, M. Oike, T. Shirai, et al. 2001. Haematopoietic cell-specific CDM family protein DOCK2 is essential for lymphocyte migration. *Nature.* **412:** 826–831.

19. McDonald, M. E., C. Li, H. Bian, B. D. Smith, M. D. Layne, and S. R. Farmer. 2015. Myocardin-related transcription factor A regulates conversion of progenitors to beige adipocytes. *Cell.* **160:** 105–118.

20. Shan, T., W. Liu, and S. Kuang. 2013. Fatty acid binding protein 4 expression marks a population of adipocyte progenitors in white and brown adipose tissues. *FASEB J.* **27:** 277–287.

21. Guo, X., S. L. Stice, N. L. Boyd, and S. Y. Chen. 2013. A novel in vitro model system for smooth muscle differentiation from human embryonic stem cell-derived mesenchymal cells. *Am. J. Physiol. Cell Physiol.* **304:** C289–C298.

22. Guo, X., P. A. Jose, and S. Y. Chen. 2011. Response gene to complement 32 interacts with Smad3 to promote epithelial-mesenchymal transition of human renal tubular cells. *Am. J. Physiol. Cell Physiol.* **300:** C1415–C1421.

23. Wang, Q., Z. Dong, X. Liu, X. Song, Q. Song, Q. Shang, Y. Jiang, C. Guo, and L. Zhang. 2013. Programmed cell death-4 deficiency prevents diet-induced obesity, adipose tissue inflammation, and insulin resistance. *Diabetes.* **62:** 4132–4143.

24. Kadowaki, T., and T. Yamauchi. 2005. Adiponectin and adiponectin receptors. *Endocr. Rev.* **26:** 439–451.

25. Yamauchi, T., J. Kamon, H. Waki, Y. Terauchi, N. Kubota, K. Hara, Y. Mori, T. Ide, K. Murakami, N. Tsuboyama-Kasaoka, et al. 2001. The fat-derived hormone adiponectin reverses insulin resistance associated with both lipoatrophy and obesity. *Nat. Med.* **7:** 941–946.

26. Kanda, H., S. Tateya, Y. Tamori, K. Kotani, K. Hiasa, R. Kitazawa, S. Kitazawa, H. Miyachi, S. Maeda, K. Egashira, et al. 2006. MCP-1 contributes to macrophage infiltration into adipose tissue, insulin resistance, and hepatic steatosis in obesity. *J. Clin. Invest.* **116:** 1494–1505.

27. Bargut, T. C., M. B. Aguila, and C. A. Mandarim-de-Lacerda. 2016. Brown adipose tissue: updates in cellular and molecular biology. *Tissue Cell.* **48:** 452–460.

28. Wellen, K. E., and G. S. Hotamisligil. 2005. Inflammation, stress, and diabetes. *J. Clin. Invest.* **115:** 1111–1119.

29. Bourlier, V., and A. Bouloumie. 2009. Role of macrophage tissue infiltration in obesity and insulin resistance. *Diabetes Metab.* **35:** 251–260.

30. Contreras, A. V., N. Torres, and A. R. Tovar. 2013. PPAR-alpha as a key nutritional and environmental sensor for metabolic adaptation. *Adv. Nutr.* **4:** 439–452.

31. Langin, D., A. Dicker, G. Tavernier, J. Hoffstedt, A. Mairal, M. Ryden, E. Arner, A. Sicard, C. M. Jenkins, N. Viguerie, et al. 2005. Adipocyte lipases and defect of lipolysis in human obesity. *Diabetes.* **54:** 3190–3197.

32. Liang, H., and W. F. Ward. 2006. PGC-1alpha: a key regulator of energy metabolism. *Adv. Physiol. Educ.* **30:** 145–151.

33. Dlasková, A., K. J. Clarke, and R. K. Porter. 2010. The role of UCP 1 in production of reactive oxygen species by mitochondria isolated from brown adipose tissue. *Biochim. Biophys. Acta.* **1797:** 1470–1476.